

Supporting Information

Luminescent Pb-free perovskites: low-cytotoxic materials for primary thermal sensing

Luan N. Passini¹, Fernando E. Maturi^{2,3}, Roberta S. Pugina⁴, Eloísa G. Hilário⁴, Marina Fontes⁵, Hernane S. Barud⁵, Luís D. Carlos², José Maurício A. Caiut⁴, and Danilo Manzani^{1}*

L. N. P., Prof. D. M.

¹São Carlos Institute of Chemistry, University of São Paulo (USP), São Carlos, SP, 13560-970, Brazil

*E-mail: dmanzani@usp.br

F. E. M., Prof. L. D. C.

²Phantom-g, CICECO – Aveiro Institute of Materials, Department of Physics, University of Aveiro, Aveiro, 3810-193, Portugal

F. E. M.

³Institute of Chemistry, São Paulo State University (UNESP), Araraquara, SP, 14800-060, Brazil

Dr. R. S. P., E. G. H., Prof. J. M. A. C.

⁴Department of Chemistry, Faculty of Philosophy, Sciences and Letters, University of São Paulo (USP), Ribeirão Preto, SP, 14040-901, Brazil

M. F., Prof. H. S. B.

⁵BioPolMat – Biopolymers and Biomaterials Research Group, University of Araraquara (UNIARA), Araraquara, SP, 14801-040, Brazil

Keywords: perovskites, lead-free perovskites, upconversion luminescence, thermometry, cytotoxicity

Table of Contents

S1. Scanning electron microscopy	2
S2. Optical properties of the co-doped In-based perovskites	3
S3. Thermometric performance of the luminescent co-doped In-based perovskites	6
S4. Energy gap and power-dependent intensity ratio	7

S1. Scanning electron microscopy

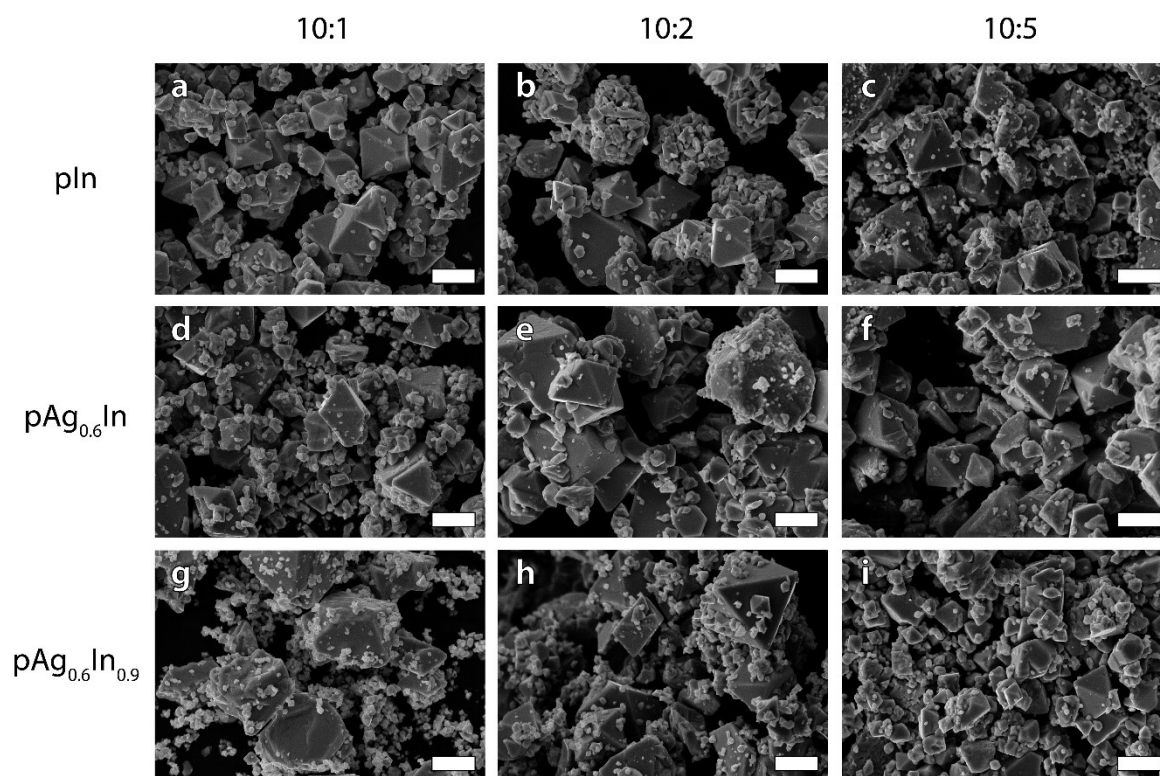


Figure S1. SEM micrographs of the pIn_{0.9} (a, b, and c), pAg_{0.6}In (d, e, and f), and pAg_{0.6}In_{0.9} (g, h, and i) perovskites co-doped with Yb³⁺/Er³⁺ at 10:1, 10:2, and 10:5 doping ratios. The scale bar is 10 μ m for all the panels.

S2. Optical properties of the co-doped In-based perovskites

Table S1. Calculated energy band gap of Ln³⁺-doped samples.

Yb ³⁺ /Er ³⁺ ratio	pIn _{0.9}		pAg _{0.6} In		pAg _{0.6} In _{0.9}	
	E_{g1} [± 0.03 eV]	E_{g2} [± 0.03 eV]	E_{g1} [± 0.03 eV]	E_{g1} [± 0.03 eV]	E_{g2} [± 0.03 eV]	
10:1	3.36	2.96	3.65	3.44	2.80	
10:2	3.40	2.99	3.65	3.38	2.95	
10:5	3.42	3.00	3.65	3.30	2.96	

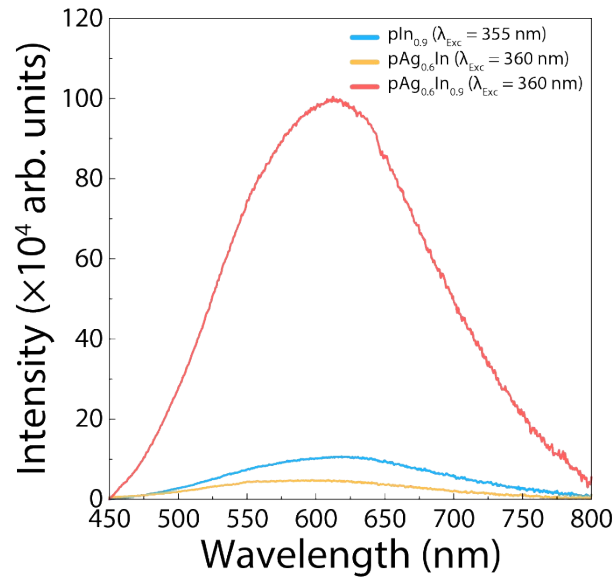


Figure S2. Comparison of the emission spectra of the pIn_{0.9} (blue), pAg_{0.6}In (yellow), and pAg_{0.6}In_{0.9} (red) samples under excitation at 355, 360, and 360 nm, respectively.

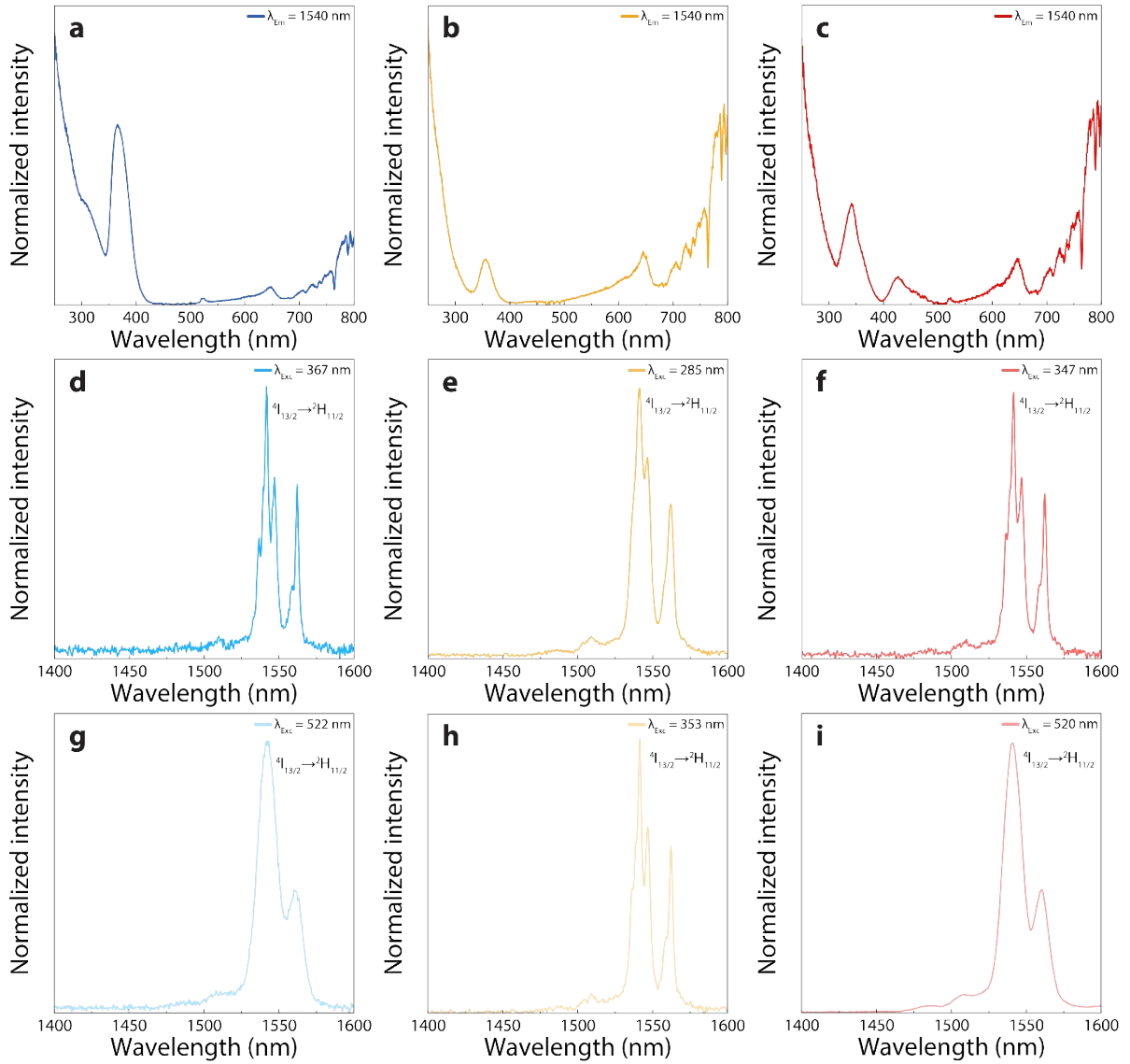


Figure S3. Excitation spectra of the (a) pIn_{0.9}, (b) pAg_{0.6}In, (c) and pAg_{0.6}In_{0.9} samples doped with Yb³⁺/Er³⁺ (10:5) monitoring the emission at 1540 nm. Emission spectra of the (d) pIn_{0.9}, (e) pAg_{0.6}In, (f) and pAg_{0.6}In_{0.9} samples doped with Yb³⁺/Er³⁺ (10:5) under excitation at 367, 285, and 347 nm, respectively. Emission spectra of the (d) pIn_{0.9}, (e) pAg_{0.6}In, (f) and pAg_{0.6}In_{0.9} samples doped with Yb³⁺/Er³⁺ (10:5) under excitation at 522, 353, and 520 nm, respectively.

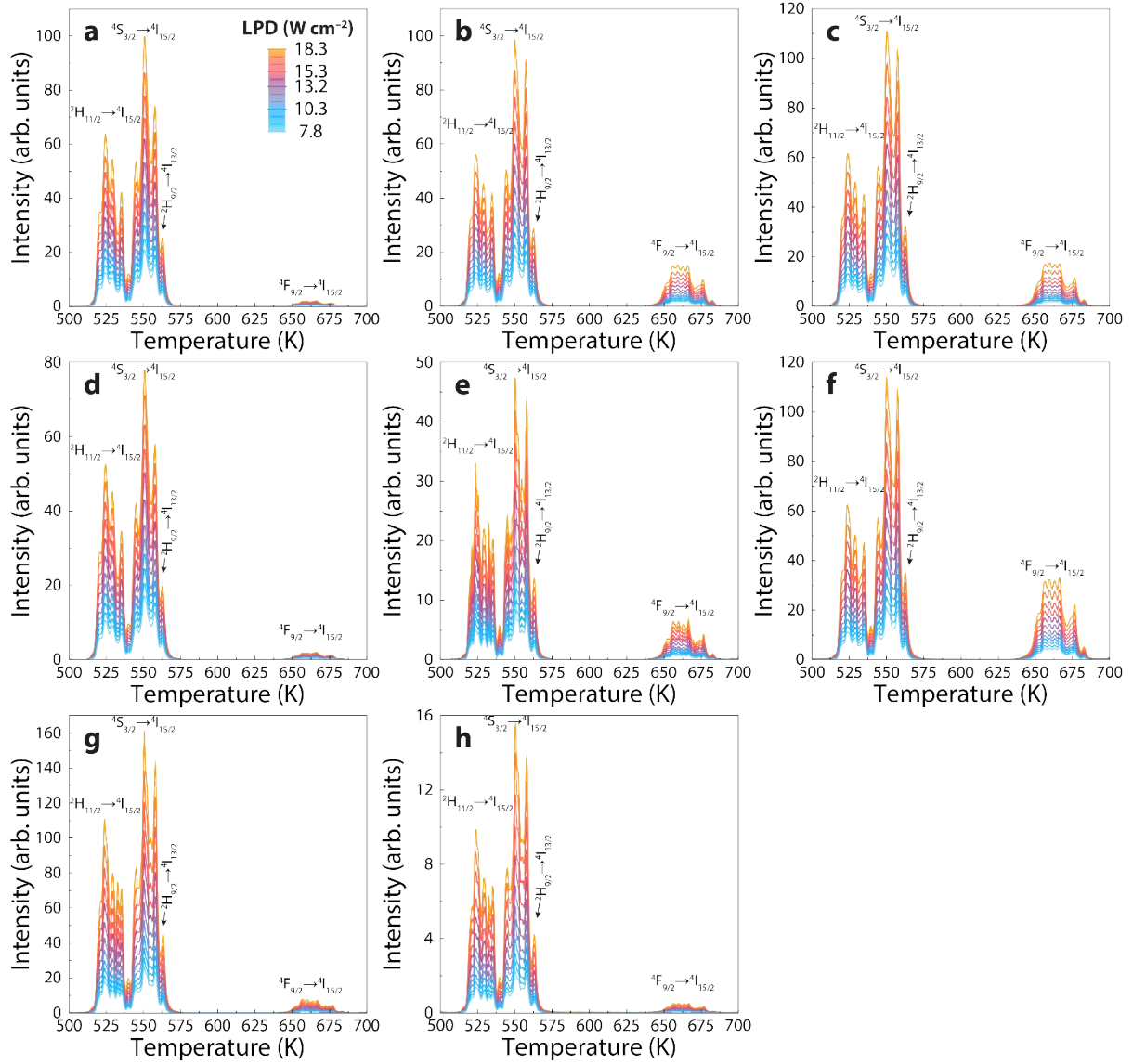


Figure S4. Upconverting emission spectra of In-based perovskite of (a) $\text{pIn}_{0.9}$, (b) $\text{pAg}_{0.6}\text{In}$, and (c) $\text{pAg}_{0.6}\text{In}_{0.9}$ samples co-doped with $\text{Yb}^{3+}/\text{Er}^{3+}$ at 10:1; (d) $\text{pIn}_{0.9}$, (e) $\text{pAg}_{0.6}\text{In}$, and (f) $\text{pAg}_{0.6}\text{In}_{0.9}$ samples co-doped with $\text{Yb}^{3+}/\text{Er}^{3+}$ at 10:2; and (g) $\text{pAg}_{0.6}\text{In}$ and (h) $\text{pAg}_{0.6}\text{In}_{0.9}$ co-doped with $\text{Yb}^{3+}/\text{Er}^{3+}$ at 10:5. All samples were excited using a 980 nm CW laser varying its laser power density (LPD) from 7.8 to 18.3 W cm^{-2} .

S3. Thermometric performance of the luminescent co-doped In-based perovskites

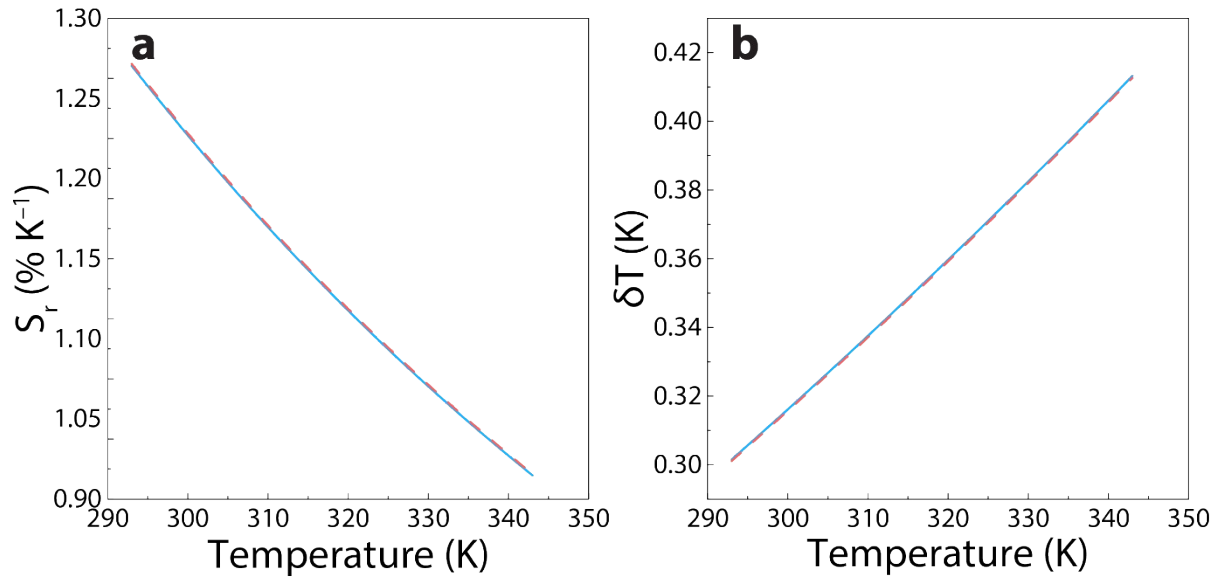


Figure S5. Thermal evolution of the (a) relative thermal sensitivity and (b) uncertainty in temperature for the obtained samples. The blue solid lines represent the results regarding the samples with a $\Delta E = 752 \pm 10 \text{ cm}^{-1}$ ($\text{pAg}_{0.6}\text{In}_{0.9}:\text{Yb}^{3+}/\text{Er}^{3+}$ (10:1), $\text{pAg}_{0.6}\text{In}_{0.9}:\text{Yb}^{3+}/\text{Er}^{3+}$ (10:5), $\text{pAg}_{0.6}\text{In}:\text{Yb}^{3+}/\text{Er}^{3+}$ (10:1), $\text{pAg}_{0.6}\text{In}:\text{Yb}^{3+}/\text{Er}^{3+}$ (10:2), $\text{pAg}_{0.6}\text{In}:\text{Yb}^{3+}/\text{Er}^{3+}$ (10:5), and $\text{pIn}_{0.9}:\text{Yb}^{3+}/\text{Er}^{3+}$ (10:1)) and the red dashed lines represent the results regarding the samples with a $\Delta E = 753 \pm 10 \text{ cm}^{-1}$ ($\text{pAg}_{0.6}\text{In}_{0.9}:\text{Yb}^{3+}/\text{Er}^{3+}$ (10:2), $\text{pIn}_{0.9}:\text{Yb}^{3+}/\text{Er}^{3+}$ (10:2), and $\text{pIn}_{0.9}:\text{Yb}^{3+}/\text{Er}^{3+}$ (10:5)).

S4. Energy gap and power-dependent intensity ratio

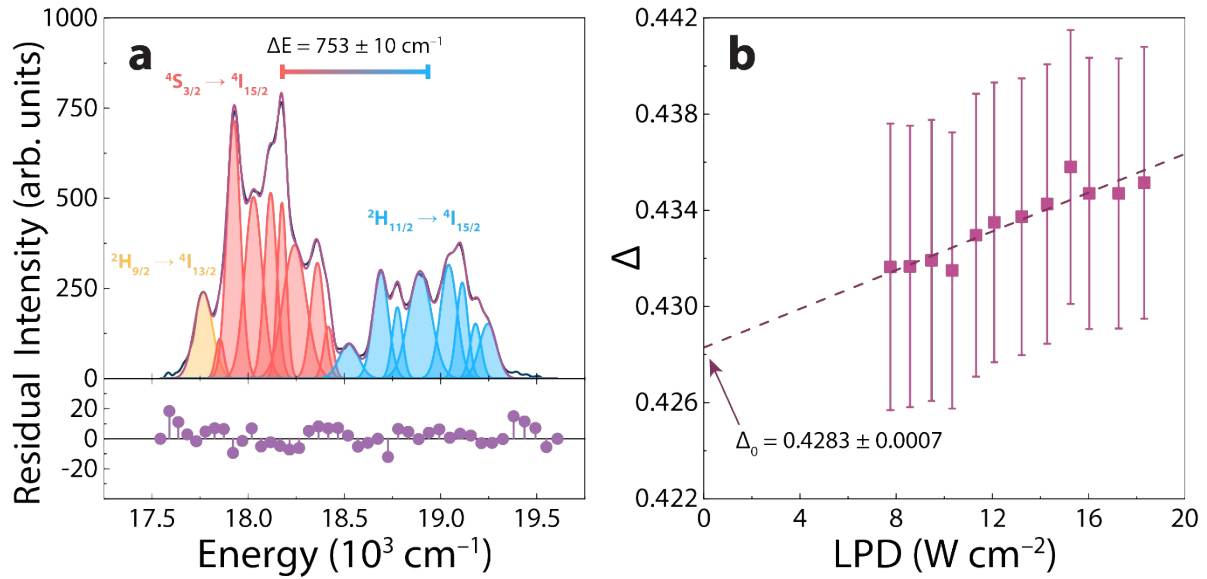


Figure S6. (a) Spectral Gaussian deconvolution illustrated for the emission spectrum of the $\text{pAg}_{0.6}\text{In}_{0.9}\text{:Yb}^{3+}/\text{Er}^{3+}$ (10:2) sample measured at 273 K and 18.3 W cm^{-2} under 980 nm excitation. The shadowed areas correspond to the Gaussian fit to the Stark components of the $^4S_{3/2} \rightarrow ^4I_{15/2}$ (red) and $^2H_{11/2} \rightarrow ^4I_{15/2}$ (blue) transitions of Er^{3+} , where their respective barycenters were used to calculate ΔE . The $^2H_{9/2} \rightarrow ^4I_{13/2}$ transition is depicted in yellow. The bottom part demonstrates the residuals of the fitting procedure. (b) Determination of Δ_0 for the $\text{pAg}_{0.6}\text{In}_{0.9}\text{:Yb}^{3+}/\text{Er}^{3+}$ (10:2) sample. The power dependence of Δ was analyzed by plotting Δ against the laser power density (LPD) of the excitation laser.